Japanese Journal of Applied
Physics

The Japan Society
of Applied Physics

Enhancement of Luminance Characteristics in Top-Emission Organic Light Emitting Diode with Cr/Al/Cr Anodes

To cite this article: Sung Mook Chung *et al* 2007 *Jpn. J. Appl. Phys.* **46** 3618

Japanese Journal of Applied Physics
Vol. 46, No. 6A, 2007, pp. 3618–3621

Enhancement of Luminance Characteristics in Top-Emission Organic Light Emitting Diode with Cr/Al/Cr Anodes

Sung Mook CHUNG, Chi-Sun HWANG, Jeong-Ik LEE, Sang Hee Ko PARK,
Yong Suk YANG, Lee-Mi DO, and Hye Yong CHU

IT Convergence-Component, Electronics and Telecommunications Research Institute,
161 Gajeong-dong, Yuseong-gu, Daejeon 305-350, Korea

(Received December 1, 2006; accepted March 15, 2007; published online June 6, 2007)

Top-emission organic light-emitting diodes (TEOLEDs) using chromium anode have been fabricated by employing two techniques: direct-current magnetron sputtering and e-beam evaporation. Atomic force microscopy and work function taken on the chromium film surfaces obtained from both techniques revealed that using dc magnetron sputtering is advantageous over e-beam evaporation in terms of surface characteristics particularly when the film is deposited. The anode having a triple-layer structure of Cr/Al/Cr was deposited on a Si wafer. The device structure of the TEOLED was Cr (20 nm)/Al (100 nm)/Cr (20 nm)/α-napthylphenylbiphenyl diamine (NPB) (60 nm)/tris(8-hydroxyquinoline) aluminum (Alq_3) (60 nm)/LiF (1 nm)/Al (2 nm)/Ag (20 nm)/NPB (200 nm). The TEOLED containing the Cr layer deposited by dc magnetron sputtering method showed higher luminance and efficiency than that containing the Cr layer deposited by e-beam evaporation. The superior device characteristics of the TEOLED containing the chromium layer deposited by dc magnetron sputtering have been investigated. [DOI: 10.1143/JJAP.46.3618]

KEYWORDS: top-emission organic light-emitting diodes, anode, sputtering, e-beam evaporation, triple layers, characteristics

1. Introduction

Transparent organic light-emitting diodes (TOLEDs) or top-emission organic light-emitting diodes (TEOLEDs) have become increasingly interesting in recent years because of their technological potential for multi color self-resolution, high contrast and high aspect ratio active matrix organic light-emitting device (AMOLED), and OLED micro displays.[1–3] The advantages of OLEDs over Flat Panel Displays are their high emission efficiency in the visible spectrum, ease of processing, and almost infinite possibility for modification.[4,5] A TEOLED electrode usually consists of transparent conducting oxides (TCO), thin metals or other combinations, such as a dot-nickel embedded indium tin oxide (ITO).[6–8] However, the high residual stress and stiffness of a metal layer or the TCO layer make it difficult to use as an electrode on a flexible substrate. For efficient hole injection, high work function materials are necessary to reduce the energy barrier between the Fermi level of the anode and the highest occupied molecular orbital (HOMO) of the adjacent organic layer. The metals previously investigated as anodes for OLEDs are Ni, Ag, Au, Cr, and Pt.[6–10] These metal films have been investigated for their high-work function and chemical stability, either as a substitute for ITO or as a thin layer deposited on highly reflective metals. In this work, the TEOLED with the Cr/Al/Cr anode on the poly(ethylene sulfone) (PES) film is a promising candidate as a flexible OLED, because of it can be bent to a substantial degree without breaking. The TEOLED anode layers have been prepared by various of methods such as sputtering, e-beam evaporation, thermal evaporation, and pulsed laser deposition.[6,8–11] It is well known that a metal thin film has the size of various crystals and the growth direction of the crystals with the deposition method or deposition conditions.[12,13] These improved film properties would ensure more advanced device performances such as enhanced luminescence efficiency and longer lifetime.[14] In this study, we have prepared the Cr anode by dc magnetron sputtering and e-beam evaporation and investigated the effects of the anode deposition methods on the TEOLED characteristics.

2. Experimental Procedure

The silicon wafer with a thermally grown silicon oxide layer was used as a substrate for the control experimental. The structure of the anode was Cr/Al/Cr and patterned by photolithography. Reflective and opaque Cr anodes were patterned by photolithography and wet etching. Al was deposited by dc magnetron sputtering. The Cr layer was grown by dc magnetron sputtering and e-beam evaporation. The base vacuums for the sputtering and e-beam evaporation were approximately 5×10^{-7} and 3×10^{-6} Torr, respectively. The edge of the anode was passivated using an organic material to prevent short failure between the cathode and the anode. Surface morphology was examined by scanning electron microscopy (SEM) and atomic force microscopy (AFM). The substrates containing patterned Cr anodes were routinely cleaned and treated with oxygen plasma at 20 W for 3 min before loading into a thermal evaporation chamber with base vacuum of 5×10^{-7} Torr. The device structure of TEOLED grown by vacuum thermal deposition was α-napthylphenylbiphenyl diamine (NPB)/tris(8-hydroxyquinoline) aluminum (Alq_3)/LiF/Al/Ag/NPB where NPB and Alq_3 were used as a hole transfer or buffer layer and an emitting layer, respectively. The multilayer of LiF (1 nm)/Al (2 nm)/Ag (20 nm) was used as a cathode. The deposition rates of the organic layers were between 0.1 and 0.2 nm/s. The sample was then transferred to another chamber without breaking the vacuum for cathode deposition. Electroluminescence spectra were obtained using a Minolta CS-1000. The current/voltage and luminescence/voltage characteristics were obtained using a current/voltage source/measure unit (Keithley 238) and a Minolta LS-100. We measured the work function using a photoelectron spectrometer (Model AC-2, RIKEN). All these TEOLEDs were measured at room temperature with glass encapsulation.

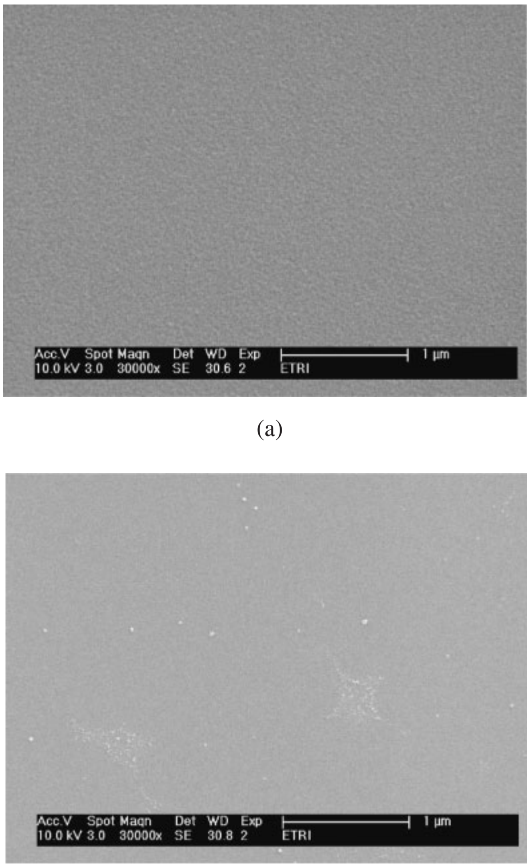

(a)

(b)

Fig. 1. SEM image of Cr/Al/Cr anodes. Cr/Al/Cr anodes deposited by sputtering (a) and e-beam evaporation (b).

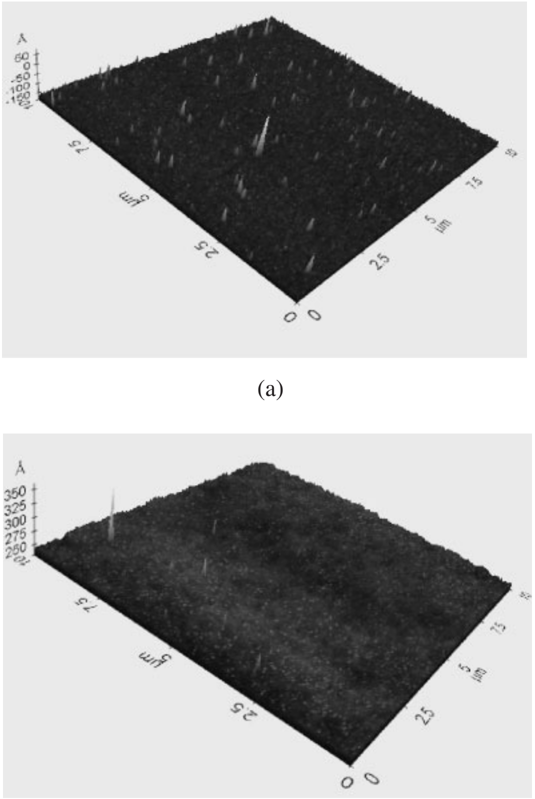

(a)

(b)

Fig. 2. AFM image of Cr/Al/Cr anodes. Cr/Al/Cr anodes deposited by sputtering (a) and (b) e-beam evaporation (b).

3. Results and Discussion

The plasma-treated Cr layer is appropriate for an anode electrode. However, the high residual stress and stiffness of the Cr layer made it difficult to use as an electrode on a flexible substrate. We have optimized Cr and Al thicknesses to prevent a possible crack of the metal film after the bending of the flexible substrate, which resulted in a Cr (20 nm)/Al (100 nm)/Cr (20 nm) structure. Al was used to make the film more flexible and to increase the conductivity and reflectivity of the anode layer. For the given anode structure, the effects of the deposition of Cr on device characteristics have been investigated on a Si wafer substrate. Figure 1 shows the SEM image of the Cr anodes on Si wafers. The surface of Cr deposited by dc magnetron sputtering on the Si wafer was very smooth compared with that deposited by e-beam evaporation on which some particles were observed. The smoother anode surface is believed to correspond to the improved characteristics of the OLED devices. The pinholes will produce a short current from the anode directly underlying the NPB and cathode, preventing the current from contributing to luminescence, and precluding luminescence at reasonable current levels; however, this is not shown on both films.[15] From the AFM study, we also found that there were some particles on the surface as shown in Fig. 2. The rms values of the Cr films deposited by sputtering and e-beam evaporation are 7.65 and 52.54 Å, respectively. Normal metal atoms during deposition find their positions along the crystal plane with the smallest surface energy and grow perpendicular to this plane. Although metal films deposited by e-beam evaporation or sputtering posses different structures from a perfect crystal, their general aspect shows some similarity.[16] From these results, we conclude that the deposition by sputtering produces a better film than that by e-beam evaporation. Some features are also known about an e-beam-deposited thin film and a sputtering-deposited thin film. E-beam deposition produces essentially line-of-sight characteristics, and for this reason it is necessary to move the substrate to sample various arrival angles. In spite of this randomization, the e-beam-deposited films grow with a columnar structure. Although substrate adhesion might be strong, the coating might exhibit poor coherence because intercolumn void space can permit gases to permeate, and the structure as a whole is subject to fracture because the bonding between columns is weak. However, sputtered coatings can also exhibit a columnar grain structure however, there is a greater capacity to affect the size of the columns. The operative parameters that determine structure are as follows kinetic energies of the sputtered atoms (in excess of $\sim$5 eV, compared with $<$1 eV for e-beam evaporation), energy transfer from energetic ions in the plasma, and scattering by the relatively high density of the gas atmosphere. These parameters prevent columnar growth by providing greater mobility on the substrate surface and scatter into many directions. Energy and gas pressure must be balanced, however, because high background pressures can lead to porous coatings, such as with argon adsorption to grain surfaces. At high bombarding

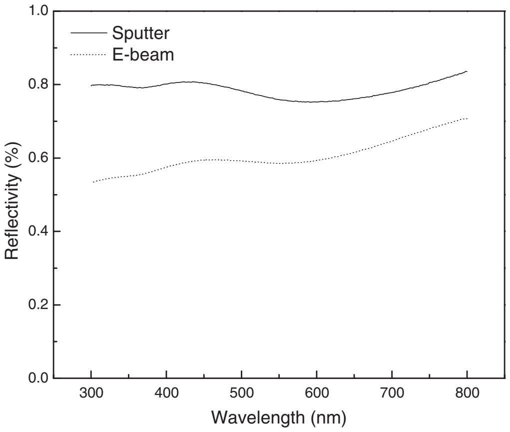

Fig. 3. Reflectance spectra of Cr/Al/Cr anodes deposited by sputtering and e-beam evaporation.

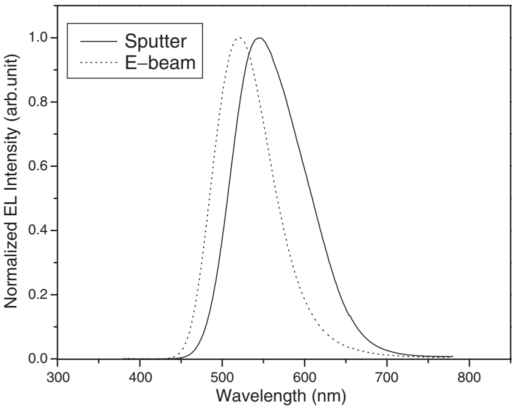

Fig. 4. Electroluminescence spectra of TEOLEDs on Si wafer.

energies near 500 eV, a columnar structure can be suppressed, and fine grained layers result.[17,18)] The sputtering would be fragmented on the substrates and it is likely that their kinetic energy leads to effective surface migration so that we may achieve an improved surface.[18–20)]

Figure 3 shows the reflectance spectra of the Cr/Al/Cr anodes deposited by sputtering and e-beam evaporation. A higher reflectance than that of a chromium single layer was obtained in the Cr/Al/Cr multilayers. In two Cr/Al/Cr multilayers, sputtering produced gave a film with a higher reflectance. The origin of the difference in reflectance is not clear but the poor surface morphology of the film grown by e-beam deposition might be related.

Figure 4 shows the EL spectra of TEOLEDs (at 20 mA/cm^2). The TEOLED containing the sputter deposited Cr anode showed an emission maximum of about 537 nm whereas the emission maximum of the TEOLED containing the e-beam evaporation-deposited Cr anode shifted to 520 nm. The EL peak appeared at 530 nm in bottom-emission OLED with Alq$_3$ based on indium tin oxide (ITO)/glass (data not shown). The difference in the emission spectra should be related to the work function of the Cr/Al/Cr layers. From this phenomenon, we can verify the concept that when work function increases in the hole transfer layer (HTL), the hole carrier hopping distance decreases and therefore is beneficial to hole current conduction, whereas electron hopping distance increases and leads to a lower electron carrier mobility. The holes injected from the HTL interface can propagate for a longer distance before recombining with electrons than the electrons that are injected from the electron transfer layer (ETL) interface. Therefore, the recombination positions shift.[21)]

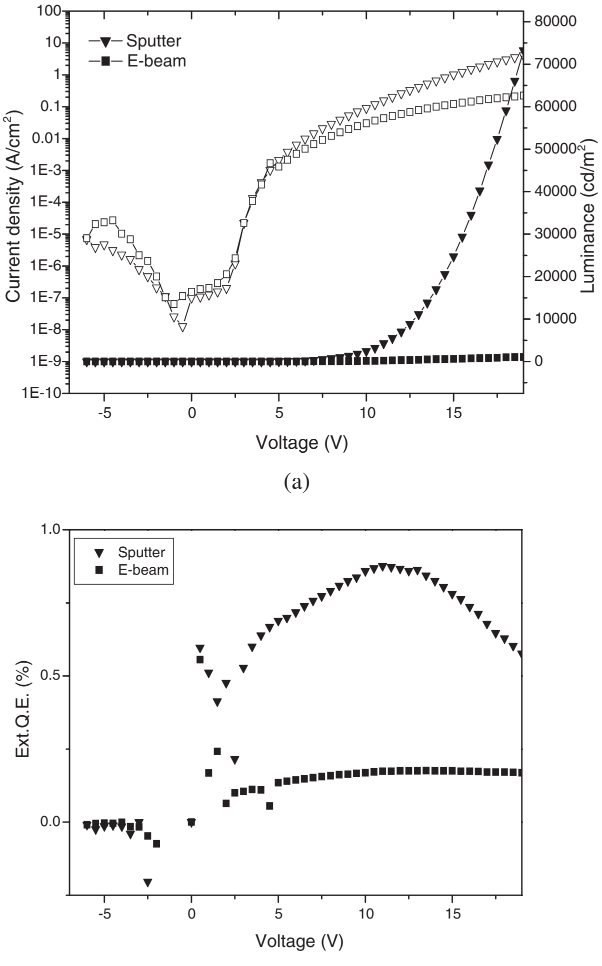

(a)

(b)

Fig. 5. (a) *J*–*V*–*L* characteristics of TEOLEDs on Si wafer and (b) external electroluminescence quantum efficiency vs voltage of TEOLEDs.

Figure 5 shows the (a) current density–voltage–luminance (*J*–*V*–*L*) characteristics of the TEOLEDs and (b) the external electroluminescence quantum efficiency vs voltage of the TEOLEDs. The maximum luminance and external quantum efficiencies of the devices containing sputtering- and e-beam-deposited anodes were about 75,000 and 300 cd/m^2, and 0.88 and 0.18%, respectively. Although the *J*–*V* characteristics were similar for both devices at a low voltage region, a higher current density was observed in the device containing the Cr anode grown by sputtering deposition at a high voltage region. According to the photoelectron spectrometer result, we obtained a work function of 5.2 eV for the as-deposited Cr film by sputtering, which is higher than that of 4.8 eV for the Cr film by e-beam evaporation. Therefore, the lower current density of the TEOLED containing the Cr anode grown by e-beam evaporation might be explained by a higher injection barrier between the anode and the hole transporting layer of NPB. The experimental results suggest that by the Ar ion bombardment

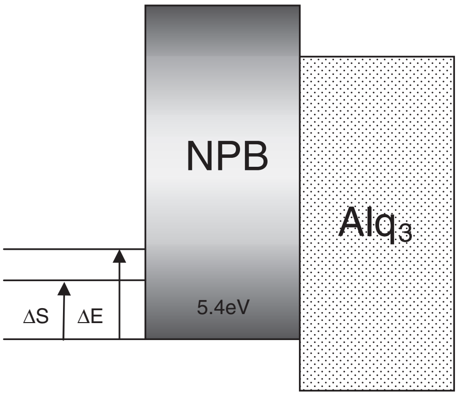

Fig. 6. Energy band diagram of TEOLED.

with controlled energy, a growing Cr thin film by dc magnetron sputtering transfers the momentum of Ar ions to the particles on the substrate, and enhances the mobility of particles, resulting in a higher packing density, i.e., a higher work function.[22–26] As for external quantum efficiency, the higher work function anode showed a better efficiency due to a lower injection barrier, which resulted in better charge balance. The high performance is attributed to the balance injection of charge carriers and the effective extraction of EL emission from the anode.

Figure 6 shows the models of an energy diagram of the TEOLEDs containing sputtering- and e-beam-deposited Cr layers. The NPB is determined to be $5.35 \pm 0.05\,\text{eV}$ using the cutoff and low balance energy onset of the HOMO.[8,25)]

By using the energy level, the following equations can be considered

$$\Phi_{\text{sputter}}\text{: } 5.2\,\text{eV}, \quad \Phi_{\text{e-beam}}\text{: } 4.8\,\text{eV}, \quad \Phi_{\text{NPB}}\text{: } 5.4\,\text{eV}$$

$$(\Phi_{\text{NPB}} - \Phi_{\text{e-beam}}) > (\Phi_{\text{NPB}} - \Phi_{\text{sputter}})$$

$$(0.6) > (0.2),$$

where Φ_{sputter} is the work function of the Cr film by direct magnetron sputtering, $\Phi_{\text{e-beam}}$ is the work function of the Cr film by e-beam evaporation, and Φ_{NPB} is the highest occupied molecular orbital level of NPB. Consequently, the luminance and turn-on voltage in TEOLEDs could be improved by the work function of the Cr anode. The enhancement of emission intensity originated from the balanced injection of electrons and holes into the TEOLEDs, as shown in Fig. 5.

4. Conclusions

Chromium anodes using direct current sputtering and e-beam evaporation have been successfully fabricated on a Si wafer. The Cr anode prepared by sputtering deposition method showed better device characteristics in terms of maximum luminance and external quantum efficiency. The enhanced device characteristics could be explained by the higher work function and reflectance of the Cr anode grown by sputtering.

Acknowledgement

The Korea Ministry of Information and Communication financially supported this work.

1) R. Cheng, C. N. Borca, N. Pilet, B. Xu, L. Yuan, B. Doudin, S. H. Liou, and P. A. Dowben: Appl. Phys. Lett. **81** (2002) 2109.
2) J. I. Lee, H. Y. Chu, H. Y. Lee, J. Y. Oh, L.-M. Do, T. Zyung, J. M. Lee, and H. K. Shin: ETRI J. **27** (2005) 181.
3) Y. Li, L. W. Tan, X. T. Hao, K. S. Ong, F. Zhu, and L. S. Hung: Appl. Phys. Lett. **86** (2005) 153508.
4) J. I. Lee, V. Y. Lee, and Robert D. Miller: ETRI J. **24** (2002) 409.
5) G. G. Qin, A. G. Xu, G. L. Ma, G. Z. Ran, Y. P. Qian, B. R. Zhang, W. X. Chen, and S. K. Wu: Appl. Phys. Lett. **85** (2004) 5406.
6) S. M. Chung, C.-S. Hwang, J.-I. Lee, S. H. Ko Park, Y. S. Yang, L.-M. Do, and H. Y. Chu: Proc. Int. 12th Int. Display Workshops in conjunction with Asia Display, 2005, p. 719.
7) C. M. Hsu, C. L. Tsai, and W. T. Wu: Appl. Phys. Lett. **88** (2006) 083515.
8) J. X. Tang, Y. Q. Li, L. S. Hung, and C. S. Lee: Appl. Phys. Lett. **84** (2004) 73.
9) C. J. Lee, R. B. Pode, D. G. Moon, and J. I. Han: Thin Solid Films **467** (2004) 201.
10) D. G. Moon, R. B. Pode, C. J. Lee, and J. I. Han: Synth. Met. **146** (2004) 63.
11) X. L. Zhu, J. X. Sun, H. J. Peng, Z. G. Meng, M. Wong, and H. S. Kwok: Appl. Phys. Lett. **87** (2005) 153508.
12) J. E. Nestell, Jr. and R. W. Christy: J. Vac. Sci. Technol. **15** (1978) 366.
13) G. C. Chi, C. J. Mogab, A. D. Burtherus, and A. G. Lehner: J. Appl. Phys. **52** (1981) 2439.
14) X. Xu, G. Yu, Y. Liu, and D. Zhu: Displays **27** (2006) 24.
15) H. Mu, H. Shen, and D. Klotzkin: Solid-State Electron. **48** (2004) 2085.
16) E. J. Ri: Met. Mater. Int. **8** (2005) 591.
17) M. C. Colton and S. Pellicori: CERAC Coat. Mater. News **9** (1999) 2.
18) D. Sanchez and S. Pellicori: CERAC Coat. Mater. News **15** (2005) 1.
19) J. Rao, K. J. Lawson, and J. R. Nicholls: Surf. Coat. Technol. **197** (2005) 154.
20) L. R. Shaginyan, A. A. Onoprienko, V. F. Britun, and V. P. Smirnov: Thin Solid Films **397** (2001) 288.
21) T. C. Lin, C. H. Hsiao, and J. H. Lee: Proc. SPIE **5397** (2005) 53971S.
22) V. E. Henrich and J. C. C. Fan: J. Appl. Phys. **46** (1975) 1206.
23) J. M. Zhao, S. T. Zhang, X. J. Wang, Y. Q. Zhan, X. Z. Wang, G. Y. Zhong, Z. J. Wang, X. M. Ding, W. Huang, and X. Y. Hou: Appl. Phys. Lett. **84** (2004) 2913.
24) H. W. Choi, S. Y. Kim, W.-K. Kim, and J.-L. Lee: Appl. Phys. Lett. **87** (2005) 082102.
25) P. He, S. D. Wang, W. K. Wong, C. S. Lee, and S. T. Lee: Appl. Phys. Lett. **79** (2001) 1561.
26) C. J. Lee, Y. I. Park, J. H. Kwon, and J. W. Park: Bull. Korean Chem. Soc. **26** (2005) 1344.